

3D Back Analysis of Karyamekar Landslide, West Java, Indonesia: Effects of Tension Crack and Rainfall on Peak and Residual Soil Shear Strength

Aisya Galuh Laksita, Fikri Faris*, Ahmad Rifa'i

Department of Civil and Environmental Engineering, Universitas Gadjah Mada, Yogyakarta, INDONESIA
Jalan Grafika No 2 Yogyakarta

*Corresponding author: fikri.faris@ugm.ac.id

SUBMITTED 27 April 2023 REVISED 12 December 2023 ACCEPTED 12 December 2023

ABSTRACT A landslide was experienced in Karyamekar Village, Cilawu District, Garut Regency, West Java, on 12 February 2021 at approximately 300 m length with a depth of 20 m, leading to a steep slope. Therefore, this study aimed to use 3D back analysis to determine soil shear strength to be subsequently applied in analyzing the possibility of further landslide with due consideration for tension crack and rainfall effect. It was also used to understand the influence of these factors on slope stability. Filled tension crack and rainfall effects were modeled using Finite Element Method (FEM) while Limit Equilibrium Method (LEM) was applied for back analysis. The results of back analysis showed that peak shear strength value of ϕ was 31.18° at a cohesion of 8.01 kPa while the residual shear strength value of ϕ was 10.35° with 2.31 kPa. The ϕ_{peak} value was found to be close to the estimated 32° , but there was a significant difference in the ϕ_{residual} which was approximated to be 30° . This discrepancy could be attributed to several factors such as the accuracy of rainfall data and geometry as well as the absence of some soil samples during the investigation. The cohesion values for peak and residual soil shear strength were considered acceptable because of the smaller values compared to the typical cohesion of SM (Silty Sand) which was set at 20° . Moreover, slope stability analyses conducted using only the effect of tension crack produced a safety factor of 0.996 while those with only the effect of rainfall had 1.172. The results showed that water pressure in tension crack had a more significant influence on slope stability compared to rain. However, it was important to state that the variation in the significance of each factor was based on the assumptions made during the analysis.

KEYWORDS Back Analysis; Landslide; Tension Crack; Rainfall; Soil Shear Strength

© The Author(s) 2024. This article is distributed under a Creative Commons Attribution-ShareAlike 4.0 International license.

1 INTRODUCTION

The accurate determination of soil shear strength parameters is becoming challenging in slope stability analysis despite the importance of these values (Sonmez et al., 1998; Lin and Chen, 2017; Zuo et al., 2022). Soil strength is defined as the resistance to shear stress based on the effective internal friction angle (Φ') and effective cohesion (c'). It normally depends on the composition of soil particles, soil water, and the compaction level of soil (ABG Creative Geosynthetic Engineering, 2021). The highest shear strength obtained through a direct shear test under a given normal load is known as peak strength and it normally reduces when the shear displacement increases. Shear strength at any displacement after the peak has been exceeded is called the post-peak strength. Meanwhile, the strength where no further loss is recorded due to the increase in displacement is known as residual (Thiel, 2001). Soil shear strength concept is shown

in Figure 1, where S_f is peak strength, S_r is residual strength, C is cohesion at peak strength, and C_r is cohesion at residual strength (Fang et al., 2020). It is important to state that peak shear strength is used only in cases of first-time slope failure (Kondalumahanthy, 2013). Meanwhile, residual shear strength is normally applied in stability analysis of ancient landslides, evaluation of reactivation potential, and understanding of progressive failure mechanisms (Chen and Liu, 2014).

Deformation in slope is typically not uniform because some sections normally experience significant deformation while others are minimal. Residual shear strength parameter is normally used in sections with large deformations while peak shear strength parameter is appropriate for those with small deformation. The limit equilibrium method does not account for the influence of deformation behavior on shear strength. This is the reason

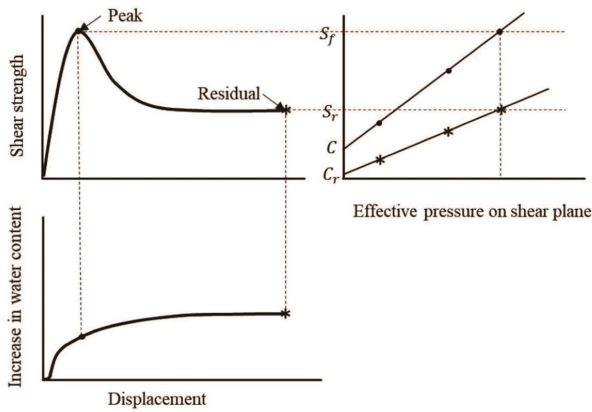


Figure 1 Concept of soil shear strength (Fang et al., 2020)

either the peak shear strength or residual shear strength value is often assumed to apply to the entire slope. However, slope safety factor has the possibility of falling between safety factor calculated using both strengths. It is important to state that actual safety factor is the same as safety factor calculated using peak shear strength when there is no deformation (Yang and Vanapalli, 2019). Soil shear strength values can be obtained through back analysis which focuses on using the reverse limit equilibrium method to calculate slope stability. This method is often applied to avoid the complexities and subjectivity of testing by making assumptions about the state of slope (Lin and Chen, 2017). Moreover, the shear strength values obtained through back analysis can be used for different things such as preventive and remedial measures, redesigning of failed slopes, or projects with similar materials (Sonmez et al., 1998). Slope conditions need to be modeled in back analysis with close similarity to the situation on the field in order to achieve accurate shear strength values. A previous study reported that groundwater table conditions significantly reduced safety factor (Ariesta, 2019). It was also discovered that infiltration was another variable influencing the reduction of safety factors in addition to the water table (Budiarti et al., 2020). However, Ariesta (2019) stated that wetting process did not significantly reduce safety factor. Another study reported that the earthquake factor on rain-affected slopes caused a decrease in safety factor due to increased pore water pressure (Faris and Fawu, 2014). Rainfall was also found to have the ability to increase the potential for landslide (Faris and Wang, 2014). On 12 February 2021, landslide occurred after heavy rainfall in Karyamekar Village, Cilawu District, Garut Regency, West Java, and

spanned approximately 300 m long with a depth of 20 m (Al Ghifari, 2021), leading to a steep slope as presented in Figure 2. Therefore, this study aimed to conduct a 3D back analysis to determine soil shear strength with due consideration for the effect of tension crack and rainfall on slope stability. The results were expected to be subsequently used to analyze the potential for further landslide. The field conditions considered include the presence of tension crack in slope and heavy rainfall before landslide occurred. This showed that the factors of tension crack, water table, and rainfall were included in back analysis.

1.1 Tension crack and groundwater table effect

The effect of water-filled tension crack was included in the modeling as the pressure head while the effect of groundwater level was the total head (Rocscience, 2018). These factors were subsequently applied in analyzing pore water pressure which was further used in back analysis.

1.2 Rainfall effect

Infiltration analysis was conducted using Green-Ampt method in order to model the effect of rainfall on slope. The method proposed an analytical simplified solution for infiltration of one-dimensional vertical rainfall with the occurrence of ponding or excess water on soil surface. Under ponding, infiltration was assumed through homogeneous soil with a uniform initial moisture distribution. The model also assumed a uniformly increasing wetting front (piston type), with constant soil matric suction, separating the maximum saturated soil from the unsaturated soil at initial moisture as presented in Figure 3a (Dolojan et al., 2021).

The original Equation of Green-Ampt is shown in Equation 1:

$$f = K_s \left(1 + \frac{\Psi \Delta\theta}{F} \right) \quad (1)$$

Where, f is infiltration capacity, K_s is the saturated hydraulic conductivity, Ψ is the matric (capillary) suction at wetting front, $\delta\theta$ is the change in volumetric water content, and F is the cumulative infiltration. Equation 1 can only be applied when the assumption of ponding at soil surface is fulfilled. Therefore, Green-Ampt Equation has been



(a) Landslide area (Prihammada and Putra, 2021)



(b) Landslide area (Google Earth, 2023)

Figure 2 Aerial photograph

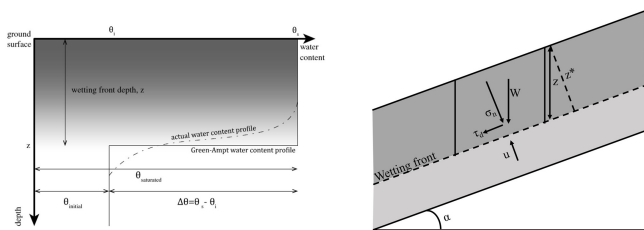


Figure 3 (a) Green-Ampt piston-type water content profile compared to the actual water content profile, where z is wetting depth, and $\theta_{initial}$ and $\theta_{saturated}$ are the initial moisture and saturated conditions, respectively, and (b) infinite slope model (Dolojan et al., 2021)

continuously developed to ensure the application in models before and after ponding conditions, on erratic rainfall, and sloping surfaces as shown in Equations 2 to 6. (Dolojan et al., 2021).

1. $f > i$: rainfall intensity is smaller than infiltration capacity. Soil can absorb all rainfall and this means there is no ponding. The cumulative infiltration, F_n , is equivalent to the cumulative rainfall. Meanwhile, infiltration capacity, f_n , is calculated using the following Equation 2, where α is slope angle, and $\Delta\theta$ is θ_s (saturated volumetric water content) - θ_i (initial volumetric water content).

$$F_n = K_s \left(\cos\alpha + \frac{\Psi \Delta\theta}{F_n} \right) \quad (2)$$

2. $f = i$: rainfall intensity is equal to infiltration capacity, leading to the initiation of ponding. The cumulative frequency, $F = F_p$, is calculated using Equation 3, and f_n is calculated using Equation 2.

$$f_p = \frac{K_s \Psi \Delta\theta}{1 - K_s \cos\alpha} \quad (3)$$

3. $f < i$: rainfall intensity is greater than infiltration capacity. Ponding and runoff occur because not all rainfall can infiltrate soil. The cumulative infiltration, F_n , is calculated using Equation 4, and f_n is calculated using Equation 2.

$$F_n = F_0 + K_s \cos\alpha \Delta t + \frac{\Psi \Delta\theta}{\cos\alpha} \left[\ln \frac{F_n \cos\alpha + \Psi \Delta\theta}{F_0 \cos\alpha + \Psi \Delta\theta} \right] \quad (4)$$

Wetting front can be calculated using Equation 5,

$$z^* = \frac{\Psi \Delta\theta}{F_n} \quad (5)$$

Where, z^* represents wetting front, normal to surface slope as presented in Figure 3b. Wetting front measured vertically from surface can be calculated using Equation 6.

$$z = \frac{z^*}{\cos\alpha} = \frac{F}{\Delta\theta \cos\alpha} \quad (6)$$

Lee et al. (2014) reported that the amount of daily rainfall and the duration of preliminary rainfall contributed to the formation of landslide mechanisms. Therefore, preliminary rainfall data obtained 3 days before the event were used in this study in line with the method adopted by Hidayat and Zahro (2020) and Yuniawan et al. (2022)

2 METHODS

2.1 Slope geometry modeling

Modeling was conducted by converting DEMNAS contour into a volume with a base at zero elevation and served as slope model before the oc-

Table 1. Soil parameters from laboratory test

Test point	Moisture content	Specific Gravity	Void Ratio	Degree of Saturation	Finer #200	Classification	γ bulk	γ dry	Direct shear		Unconfined
	wN, (%)	Gs	e	Sr, (%)	(%)				Unified	$\phi(o)$	c, (kg cm ⁻²)
P-3	49.46	2.60	1.48	87.18	18.21	SM	1.57	1.05	31.27	0.01	-

Table 2. Green-Ampt input parameter

K_s (cm h ⁻¹)	A (o)	Ψ (cm)	θ_s (cm ³ cm ⁻³)	θ_i (cm ³ cm ⁻³)	$\Delta\theta$ (cm ³ cm ⁻³)
13.64	19.80	0.44	1.53	1.11	0.42

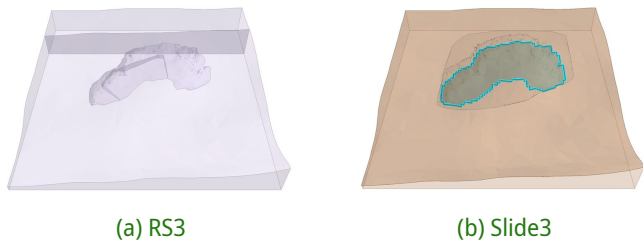


Figure 4 Model

currence of landslide. The dimensions of tension crack, including length and width, were parameterized based on aerial photographs provided by PVMBG. The depth of tension crack was simulated until it intersected with the slip surface. In RS3 software, a novel plane was generated to accommodate a pressure head mirroring the depth of tension crack in order to facilitate the integration of realistic conditions into the model. Slope geometry in RS3 and Slide3 software are presented in the following Figure 4. Moreover, soil parameters applied to the model are listed in Table 1.

2.2 Landslide back analysis

Back analysis was conducted to determine the parameters of shear strength and this was achieved through the application of the finite element and limit equilibrium methods.

2.2.1 Finite element method (FEM)

Finite element method (FEM) was used to model the pore water pressure on slope affected by groundwater table and water-filled tension crack. The depth used for the water table was 15 m and modeled as a total head of 25 m with surface elevation of 40 m from the datum. The drainage was observed from the field to have been damaged due to ground movement before landslide. This further

had a quite complex effect as shown by the need to provide additional load to the water pressure on slope. The influence was also observed from the extension of tension crack near the drainage path. This condition led to the assumption that tension crack was filled with water. The fully saturated tension crack was modeled as a pressure head of 7 m based on its depth up to the sliding plane. Moreover, the area of tension crack was adjusted to PVMBG ground movement report as shown in Figure 5.

Pore water pressure was analyzed using Rocscience RS3 software based on soil hydraulic parameters such as permeability coefficient, initial moisture, moisture at saturation, and soil type. The values of these parameters were obtained through Philip-Dunne permeability test conducted in the field as shown in Tables 1 and 2.

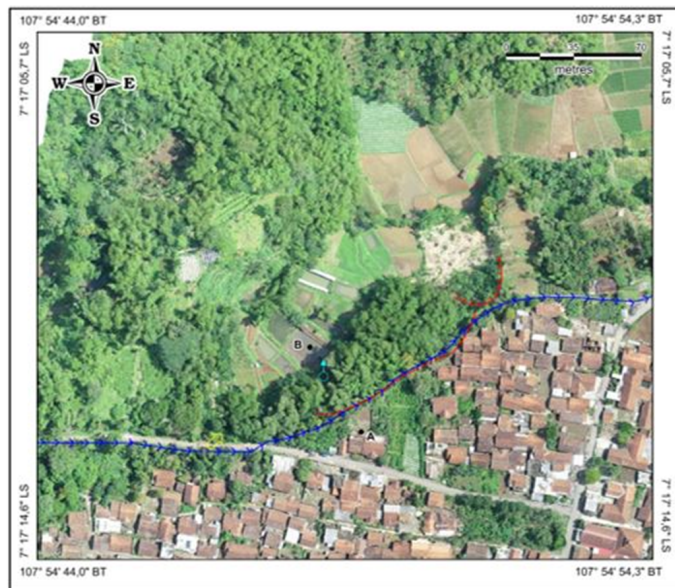
The results obtained from the hydraulic computations used to determine pore water pressure are presented in the following Figure 6. The results were later exported as pore water pressure grid for slope stability analysis using the limit equilibrium method in Rocscience Slide3 software.

2.2.2 Limit equilibrium method (LEM)

The effect of rainfall was considered as infiltration causing the development of a saturated soil layer in slope stability analysis. The depth of the saturated soil layer was calculated using Green-Ampt infiltration in Equations 2 to 6 based on the parameters listed in Tables 1 and 2. Infiltration was analyzed three days before the event through wetting depth analysis conducted using Green-Ampt infiltration method. The results presented in Figure 7 showed that wetting depth was approximately 3 cm.

2.3 Back analysis to obtain shear strength

The analysis was continued by determining landslide according to the area measured on the field



Situation Map of Creeping in Cipager Karyamekar, Cilawu, Garut, West Java

Legend:





-  Old landslide
-  Crack path
-  Drainage channel diversion location
Arrow indicates direction of diversion
-  Drainage channel

Figure 5 Creeping situation map of Cipager, Karyamekar (Kementrian ESDM Badan Geologi PVMBG, 2020)

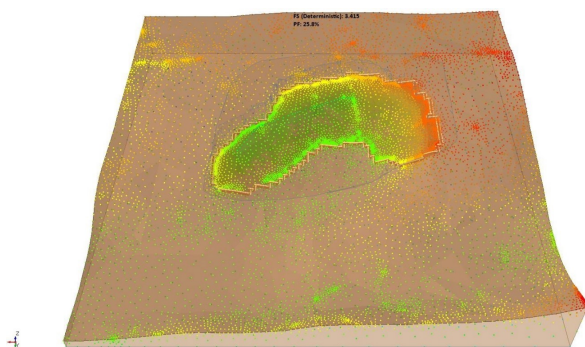


Figure 6 Pore water pressure analysis result

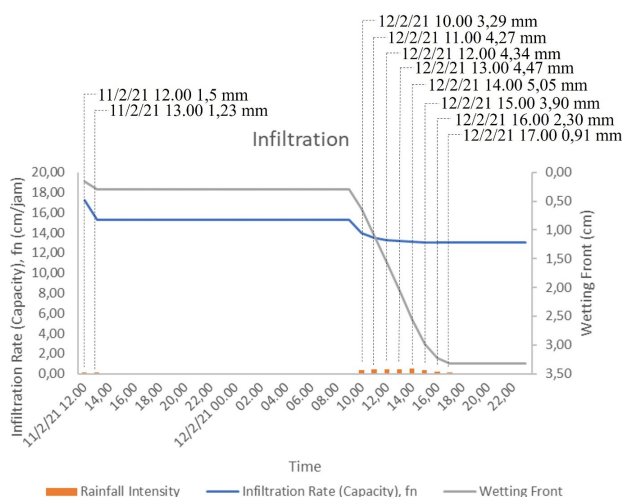


Figure 7 Green-Ampt infiltration analysis result chart

while landslide slip surface was defined according to the contours obtained from the drone capture. Moreover, Slide3 software was also used to search for a combination of soil shear strength param-

eters in order to determine the specific safety factor for slope. This step was followed by the activation of the statistical feature in the project setting to achieve the statistical analysis of soil shear strength. The process focused on inputting the laboratory values as initial values and using the software to determine several possible combinations of soil shear strength. The initial value of ϕ inputted in the software was 31.27° obtained from laboratory test results. Cohesion value was found to be 1 kPa from the laboratory test but the value inputted was >1 kPa because a percent of fine grains classified as silty sand or SM was identified in the results. This consideration led to the selection of 20 kPa as the maximum cohesion value in line with the methods used by Dysli (2001).

3 RESULTS

Residual shear strength was obtained through back analysis of slope section that collapsed on 12 February 2021 because soil experienced large deformations (Yang and Vanapalli, 2019). Back analysis was performed by defining the slip surface in the modeling according to the field conditions. Moreover, Slide3 software was used to provide different residual $c-\Phi$ combinations with several slope safety factor values. Some points are presented in Figure 8 with different colors to show the combination of c and Φ , and similar safety factor value of 0.95-0.97 was obtained. The values were used because the slope in the field had failed,

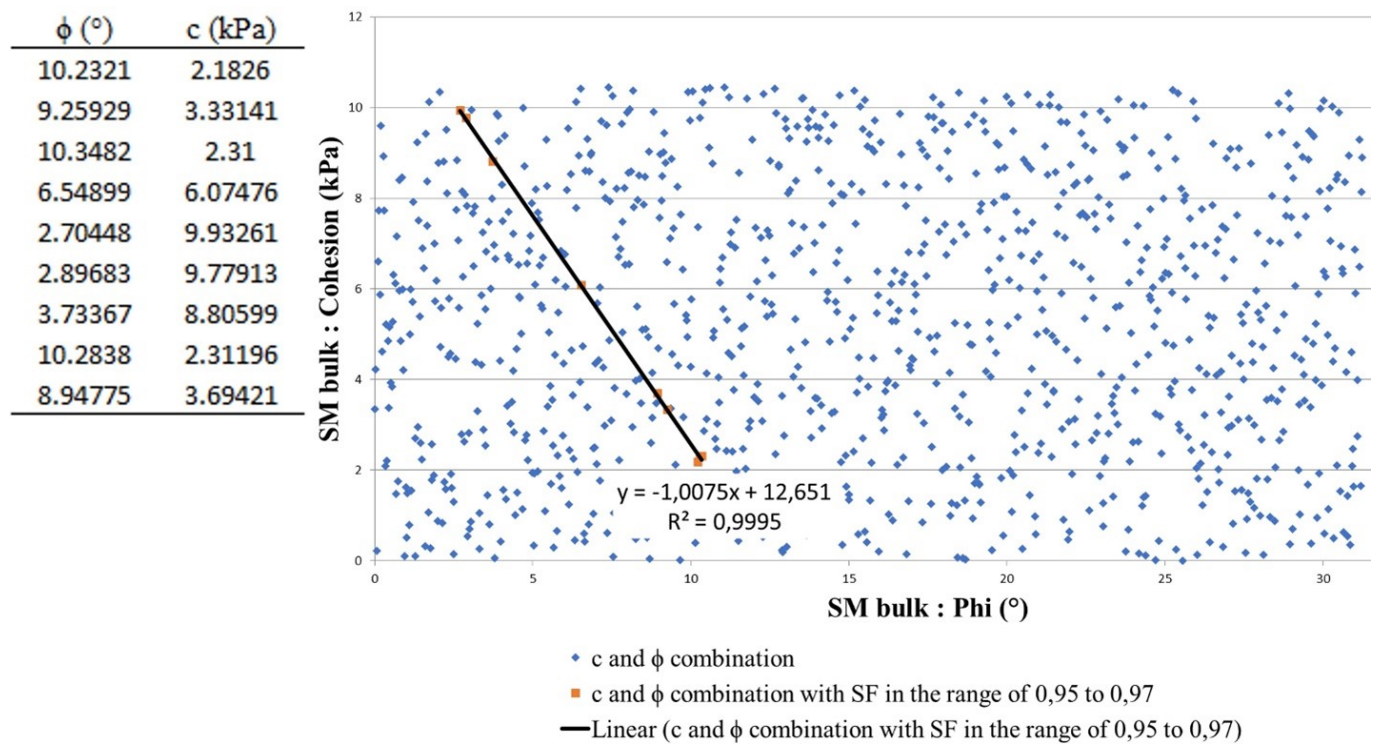


Figure 8 c- ϕ residual combination

thereby indicating the safety factor was <1.00.

Figure 8 shows the combination where one of the parameters, c or Φ , is more dominant. The single value used as residual shear strength was selected through the application of two combinations in the table to the initial slope in the model before landslide as well as the combination with the highest Φ value and the one with the highest c value. The legend was set to ensure the uppermost color contour, which was dark blue, showed safety factor of 0.95 while the other colors had a lesser value. Figure 10 shows the difference in landslide area expected when a combination of shear strength with dominant Φ value or a combination with dominant c value was used. The modeled landslide area represented using other colors apart from dark blue is observed to be closer to the field situation shown by the shaded part when using the dominant Φ combination compared to the dominant c value. This showed that residual shear strength from the combination of Φ at 10.35° and c at 2.31 kPa was used.

Landslide back analysis was conducted again to determine shear strength of slope that has not failed. The purpose was to produce peak shear strength value since slope has not been deformed in the area. This was achieved by testing slope

model from the moment after landslide up to when the safety factor ≥ 1.00 was obtained. The results presented in Figure 9 showed some points with different colors, implying the combinations of c and Φ of soil had the same safety factor values of 1.00 to 1.10. Back analysis was also applied to validate peak strength values produced through the laboratory test (Thiel, 2001). This was achieved using the value that was closest to the 31.18° in the laboratory test with cohesion value of 8.01 kPa. Moreover, peak shear strength value was also validated through slope stability analysis using the previous model, and slope was found to be safe against landslide with a minimum safety factor of 1.08, as shown in Figure 11. The result showed there was no landslide on the modeled slope in line with the field conditions. Therefore, peak shear strength modeled was considered relevant for slope shear strength in further landslide potential analysis.

4 DISCUSSION

The peak friction angles obtained were observed to be close to the values estimated by Ortiz et al. (1986) in the technical note presented by ABG Creative Geosynthetic Engineering (2021) for fine-grained uniform sand. This classification was selected because it was closest to the field soil clas-

ϕ (°)	c (kPa)	35.6254	6.10343
32.918	5.75187	32.056	7.38118
33.7254	6.3208	34.5696	4.37512
32.373	9.07222	36.2281	5.2601
34.2215	5.91641	36.9837	3.89416
36.1167	4.53748	31.5357	7.34292
35.267	4.98805	35.8197	4.61034
30.1743	10.1865	34.0668	6.61708
36.8001	4.91117	35.1744	4.28565
31.1787	8.01213	31.8967	6.75284
31.4787	8.63655	34.908	5.81198
31.0552	9.38236	29.7459	10.1323
31.8521	7.06001	32.4658	8.76582
32.4658	8.76582	33.6404	6.71397
32.0869	6.79291	31.4823	7.13885
31.4823	7.13885	30.9753	8.88919
30.9753	8.88919	35.6254	6.10343
35.6254	6.10343	36.0911	4.88119

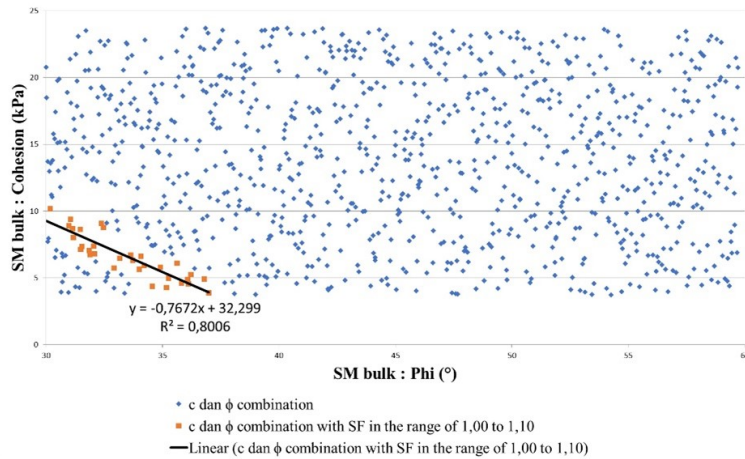
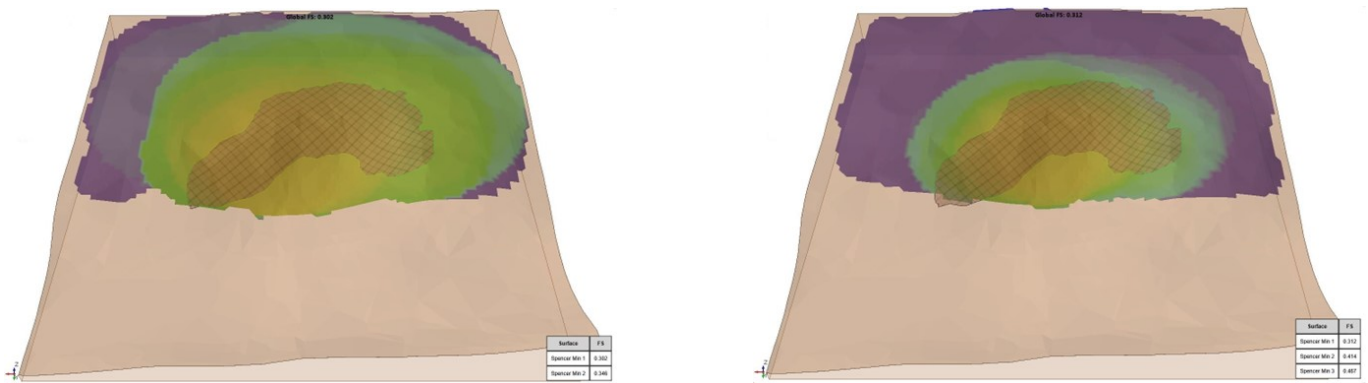


Figure 9 c-φ peak combination



(a) Combination of shear strength with the largest c

(b) Combination of shear strength with the largest φ

Figure 10 Application of residual shear strength on Slide3

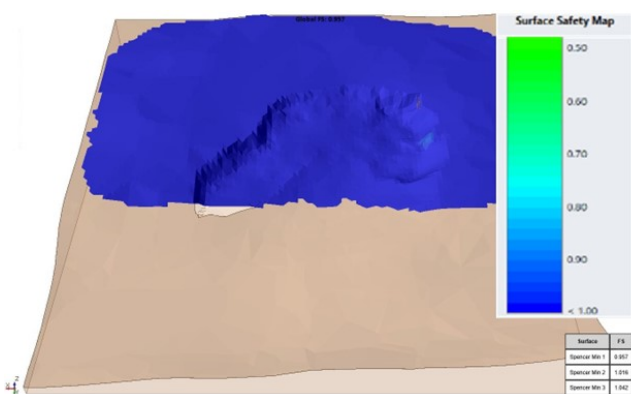


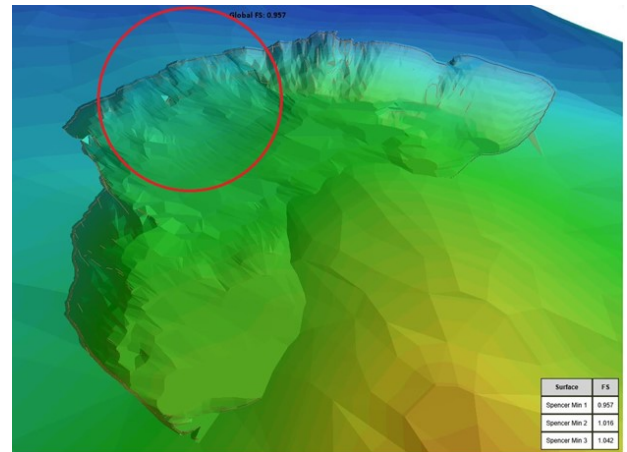
Figure 11 Landslides did not occur in the model to which the peak shear strength of back analysis was applied

sification of silty sand or SM. The laboratory and modeled soil friction angles were discovered in this study to be 31.27° and 31.18°, respectively, and these were not too far from the φ_{peak} shear

strength estimated by Ortiz et al. (1986) to be 32° with proof that SF from the model was 1,08. Moreover, the cohesion value was considered acceptable because it was smaller than the 20° found in SM soils (Dysli, 2001). A significant difference was identified in the value of soil φ residual which was reported by Ortiz et al. (1986) to be 30° while the value obtained based on the model was 10.35°. This showed that the back analysis value was significantly smaller than the estimated value. A possible reason was the usage of a smaller residual internal friction angle in the model compared to the value used by Ortiz et al. (1986). This showed that the conditions applied in the model had less significant influence on the collapse of slope. The less significance was proven by the fact that residual φ obtained was required to be very small for slope to fail. Moreover, the gaps identified between the re-



(a) Aerial photos



(b) Model geometry

Figure 12 Comparison between the south slope

sults and the field conditions were associated with several assumptions:

1. This study used rainfall data from satellite recording on GSMaP rain map with an accuracy of 0.1° latitude/longitude or equivalent to 11.1 km. The data was used because the closest rainfall station that provided data was nearly 11 km away, and the maximum value recorded was lower than those from the satellite. This reason was also supported by the results of Rifai et al. (2022) that the application of satellite rainfall data for landslide thresholds was better than using data from one local rainfall station in the study area. However, the 11 km distance covers an extensive area and this means rainfall from one point to another in an 11 km radius is probably different. The distance can lead to the possibility that rainfall in the field is greater than rainfall in the model.
2. Drainage has a complex role in contributing additional water stress to slope. Therefore, tension crack was assumed in this study to be filled with water because it was adjacent to the area of the damaged drainage as presented in Figure 5. This assumption used was the worst-case scenario due to the water pressure in tension crack.
3. Landslide geometry modeled was different from the aerial photographs of the area. This is observed from Figure 12 where slope appears steeper than the contour from the DEM drone in the aerial photo. These differences

are possibly due to the variations in the accuracy of DEMs because DEMNAS obtained from the BIG web has a resolution of 8 m while the drone DEM has a resolution of 0.3 m which can reduce the accuracy level of the model. The marked section shows that slope on the south side is steep but the drone DEM shows it is flatter. Meanwhile, steep slopes have the ability to significantly influence collapse more than flat slopes.

4. There was no soil boring or sounding test at the study area, leading to the usage of the same soil parameters at all depths. This could have led to overestimated or underestimated soil shear strength at certain depths or areas. Meanwhile, an underestimated shear strength has a more significant effect on slope failure.

Stability analysis was conducted to determine the effect of rainfall and tension crack on slope stability by eliminating one of these factors. The consideration of only tension crack produced safety factor of 0.996 while rainfall had 1.172. The results showed that the water pressure in tension crack had a more significant influence on slope stability compared to rainfall. This was in line with the assumption that water was considered to have filled tension crack in the worst-case scenario condition while rainfall only provided wetting depth of 3 cm as presented in Figure 7. The influence of each factor was different based on the variations in the assumptions used. This showed that accurate data was needed to make the assumptions considered

most suitable to the field conditions.

5 CONCLUSION

In conclusion, landslide back analysis produced peak shear strength with Φ at 31.18° and c at 8.01 kPa while residual shear strength was 10.35° and 2.31 kPa, respectively. The Φ peak values were proved to be close to the 32° estimated by Ortiz et al. (1986) in the technical note by ABG Creative Geosynthetic Engineering (2021) for fine-grained uniform sand. Meanwhile, the Φ residual was significantly different as shown by the 30° estimated by Ortiz et al. (1986). This variation was due to several factors, including rainfall data covering a larger area, geometry differences due to DEM accuracy before and after the landslide, and the absence of investigation on soil borings and soundings. However, cohesion values for peak and residual soil shear strength were considered acceptable due to the small values recorded compared to the 20° required in SM soil (Dysli, 2001). Filled tension crack was discovered to have a more significant influence than rainfall on slope stability. This was shown by safety factor of 0.996 recorded when only the effect of tension crack was considered compared to the 1.12 observed for rainfall. The lesser value recorded for rainfall was because the study area did not have sufficient rainfall as observed from wetting front depth of 3 cm which was insignificant compared to the 20 m reported for landslide. Moreover, the drainage showed a very complex behavior in providing additional water pressure on slope. This was associated with the assumption that the water from the drainage flowed into tension crack, causing excess pressure and placing slope in a worst-case scenario. The influence of each factor was different based on the variations in the assumptions used. This showed that accurate data was needed to make the assumptions considered best suited to the field conditions.

DISCLAIMER

The authors declare no conflict of interest.

AVAILABILITY OF DATA AND MATERIALS

All data are available from the author.

REFERENCES

- ABG Creative Geosynthetic Engineering (2021), 'SOIL PROPERTIES: Shear Strength'.
- Al Ghifari, S. (2021), 'Dua rumah tertimbun dan 19 lainnya terancam longsor di Cilawu Garut'. Accessed: 14 March 2023.
URL: <https://jabar.tribun-news.com/2021/02/14/dua-rumah-tertimbun-dan-19-lainnya-terancam-longsor-di-cilawu-garut>
- Ariesta, D. (2019), 'The effect of initial groundwater table and rainfall wetting towards slope stability (case study of landslide in tangkil hamlet, Banaran Village, Pulung Subdistrict, Ponorogo Regency)', *Journal of the Civil Engineering Forum* 5(2), 149.
URL: <https://doi.org/10.22146/jcef.43804>
- Budiarti, P. W., Fathani, T. F. and Faris, F. (2020), Analysis of rainfall-triggered landslide in Baleagung Village, Magelang Regency, Central Java, in 'E3S Web of Conferences', EDP Sciences.
URL: <https://doi.org/10.1051/e3sconf/202020001001>
- Chen, X. P. and Liu, D. (2014), 'Residual strength of slip zone soils', *Landslides* 11(2), 305–314.
URL: <https://doi.org/10.1007/s10346-013-0451-z>
- Dolojan, N. L. J., Moriguchi, S., Hashimoto, M. and Terada, K. (2021), 'Mapping method of rainfall-induced landslide hazards by infiltration and slope stability analysis: A case study in Marumori, Miyagi, Japan, during the october 2019 typhoon hagibis', *Landslides* 18(6), 2039–2057.
URL: <https://doi.org/10.1007/s10346-020-01617-x>
- Dysli, M. (2001), *Recherche Bibliographique Et Synthèse Des Corrélations Entre Les Caractéristiques Des Sols*.
- Fang, C., Shimizu, H., Nishiyama, T. and Nishimura, S. I. (2020), 'Determination of residual strength of soils for slope stability analysis: State of the art review', *Reviews in Agricultural Science* 8, 46–57.
URL: <https://doi.org/10.7831/ras.8.046>
- Faris, F. and Fawu, W. (2014), 'Investigation of the initiation mechanism of an earthquake-induced landslide during rainfall: A case study of the Tandikat Landslide, West Sumatra, Indonesia'.
URL: <https://doi.org/10.1186/s40677-014-0012-3>

Faris, F. and Wang, F. (2014), 'Stochastic analysis of rainfall effect on earthquake-induced shallow landslide of Tandikat, West Sumatra, Indonesia', *Geoenvironmental Disasters* **1**(1).

URL: <https://doi.org/10.1186/s40677-014-0012-3>

Google Earth (2023). Accessed: 15 April 2023.

URL: <https://earth.google.com/web/@-7.28627011,107.91367114,969.42042403a,387.61389729d,35y,0h,0t,0r>

Hidayat, R. and Zahro, A. A. (2020), 'Penentuan ambang curah hujan untuk memprediksi kejadian longsor', *JURNAL SUMBER DAYA AIR* **16**(1), 1–10.

URL: <https://doi.org/10.32679/jsda.v16i1.483>

Kementrian ESDM Badan Geologi PVMBG (2020), 'Laporan pemeriksaan gerakan tanah di Kec. Cilawu, Kabupaten Garut, Provinsi Jawa Barat'. Accessed: 30 December 2022.

Kondalamahanthy, A. K. (2013), 2D and 3D Back Analysis of the Forest City Landslide (South Dakota), PhD thesis.

URL: <https://doi.org/10.31274/etd-180810-2963>

Lee, M. L., Ng, K. Y., Huang, Y. F. and Li, W. C. (2014), 'Rainfall-induced landslides in Hulu Kelang area, Malaysia', *Natural Hazards* **70**(1), 353–375.

URL: <https://doi.org/10.1007/s11069-013-0814-8>

Lin, H. and Chen, J. (2017), 'Back analysis method of homogeneous slope at critical state', *KSCE Journal of Civil Engineering* **21**(3), 670–675.

URL: <https://doi.org/10.1007/s12205-016-0400-1>

Ortiz, J., Serra, J. and Oteo, C. (1986), *Curso Aplicado de Cimentaciones*, 3 edn, Colegio Oficial de Arquitectos de Madrid, Madrid.

URL: <https://doi.org/10.5281/zenodo.1234567>

Prihamanda, B. A. and Putra, Y. M. P. (2021), 'Menanti relokasi rumah terdampak longsor di Cilawu Garut'. Accessed: 28 December 2022.

URL: <https://www.republika.co.id/berita/qq7l45284/menanti-relokasi-rumah-terdampak-longsor-di-cilawu-garut>

Rifai, A., Andika Yuniawan, R., Faris, F., Subiyantoro, A., Sidik, V. and Prayoga, H. (2022), Performance of rainfall satellite threshold to predict

landslide events in Girimulyo District, in '2022 IEEE International Conference on Aerospace Electronics and Remote Sensing Technology, ICARES 2022 - Proceedings', Institute of Electrical and Electronics Engineers Inc.

URL: <https://doi.org/10.1109/ICARES56907.2022.9993592>

Rocscience (2018), 'Add groundwater boundary condition'. Accessed: 12.06.23.

URL: <https://www.rocscience.com/help/rs3/documentation/groundwater-2/steady-state/add-groundwater-boundary-condition>

Sonmez, H., Ulusay, R. and Gokceoglu, C. (1998), 'A practical procedure for the back analysis of slope failures in closely jointed rock masses'.

URL: [https://doi.org/10.1016/S0148-9062\(98\)00045-9](https://doi.org/10.1016/S0148-9062(98)00045-9)

Thiel, R. (2001), 'Peak vs residual shear strength for landfill bottom liner stability analyses'.

URL: [https://doi.org/10.1061/\(ASCE\)1090-0241\(2001\)127:6\(451\)](https://doi.org/10.1061/(ASCE)1090-0241(2001)127:6(451))

Yang, X. and Vanapalli, S. (2019), 'Slope stability analyses of outang landslide based on the peak and residual shear strength behavior', *Gongcheng Kexue Yu Jishu/Advanced Engineering Science* **51**(4), 55–68.

URL: <https://doi.org/10.15961/j.jsuese.201900273>

Yuniawan, R. A., Rifa'i, A., Faris, F., Subiyantoro, A., Satyaningsih, R., Hidayah, A. N., Hidayat, R., Mushthofa, A., Ridwan, B. W., Priangga, E., Muntohar, A. S., Jetten, V. G., van Westen, C. J., Den Bout, B. V. and Sutanto, S. J. (2022), 'Revised rainfall threshold in the Indonesian landslide early warning system', *Geosciences (Switzerland)* **12**(3).

URL: <https://doi.org/10.3390/geosciences12030129>

Zuo, S., Zhao, L., Deng, D., Han, Z., Zhao, B. and Zhao, Z. (2022), 'Back analysis of shear strength parameters for progressive landslides: Case study of the Caifengyan landslide, China', *Bulletin of Engineering Geology and the Environment* **81**(1).

URL: <https://doi.org/10.1007/s10064-021-02507-9>